

Formation of pyrite (FeS₂) thin films by thermal sulfurization of dc magnetron sputtered iron

R. J. Soukup, P. Prabukanthan, N. J. Ianno, A. Sarkar, C. A. Kamler et al.

Citation: *J. Vac. Sci. Technol. A* **29**, 011001 (2011); doi: 10.1116/1.3517739

View online: <http://dx.doi.org/10.1116/1.3517739>

View Table of Contents: <http://avspublications.org/resource/1/JVTAD6/v29/i1>

Published by the AVS: Science & Technology of Materials, Interfaces, and Processing

Additional information on *J. Vac. Sci. Technol. A*

Journal Homepage: <http://avspublications.org/jvsta>

Journal Information: http://avspublications.org/jvsta/about/about_the_journal

Top downloads: http://avspublications.org/jvsta/top_20_most_downloaded

Information for Authors: http://avspublications.org/jvsta/authors/information_for_contributors

ADVERTISEMENT



 Advance your technology or engineering career using the **AVS Career Center**, with hundreds of exciting jobs listed each month!

<http://careers.avs.org>



Formation of pyrite (FeS₂) thin films by thermal sulfurization of dc magnetron sputtered iron

R. J. Soukup,^{a)} P. Prabukanthan, N. J. Ianno, A. Sarkar, C. A. Kamler, and D. G. Sekora
Department of Electrical Engineering, University of Nebraska-Lincoln, Lincoln, Nebraska 68588-0511

(Received 29 March 2010; accepted 25 October 2010; published 3 January 2011)

Iron films deposited by direct current magnetron sputtering onto glass substrates were converted into FeS₂ films by thermal sulfurization. Experiments were carried out to optimize the sulfurization process, and the formation of FeS₂ thin films was investigated under different annealing temperatures and times. High quality FeS₂ films were fabricated using this process, and single phase pyrite films were obtained after sulfurization in a sulfur and nitrogen atmosphere at 450 °C for 1 h. Film crystallinity and phase identification were determined by using x-ray diffraction. The cubic phase pyrite films prepared were *p*-type, and scanning electron microscopy studies exhibited a homogeneous surface of pyrite. The authors have found that the best Ohmic contact for their pyrite thin films, using inexpensive metals, was Ni. The following were chosen for the study: Al, Mo, Fe, and Ni, and the one that led to the lowest resistance, 333 Ω, was Ni. © 2011 American Vacuum Society. [DOI: 10.1116/1.3517739]

I. INTRODUCTION

Much interest has been focused on highly absorbing and photoactive semiconductors to be used in ultrathin and flexible solar cells. As an optoelectronic or photovoltaic material, cubic (pyrite) FeS₂ is receiving growing attention because of its promising potential for such applications.^{1,2} In addition, its abundant, inexpensive, and nontoxic components are also the reason for the enormous interest in pyrite as an absorber material for thin film solar cells.³ Many techniques for thin film preparation have been investigated in order to obtain suitable pyrite films.^{4–14} These studies have indicated that the character and quality of the films are strongly dependent on the process parameters used in preparing the films. Therefore, special attention must be devoted to the effects of these process parameters on the formation of pyrite thin films prepared by synthetic techniques. Despite this, the conversion efficiency of FeS₂ solar cells has not exceeded 3%.¹ The reason for the low value can be attributed to phase impurity and contact problems, among other things. That is, FeS₂ can crystallize not only into a cubic pyrite structure, but also into an orthorhombic metastable marcasite structure. Therefore, new and improved techniques are needed to resolve these problems. Moreover, a simple method should also be developed such that the growth of pyrite thin films can be made onto large areas.

In this article, an inexpensive alternative method based on the thermal sulfurization of metallic Fe films deposited using direct current magnetron sputtering is described. The experimental conditions required for growing FeS₂ films and the influence of the sulfurization parameters on their structural, optical, morphological, and electrical properties are discussed. Variations of the deposition and sulfurization tech-

niques listed above were used to seek the best possible method to fabricate a thin film iron pyrite solar cell absorber.

II. EXPERIMENTAL PROCEDURES

Fe films were deposited using direct current (dc) sputtering of an Fe target (99.99% pure) onto soda lime glass substrates at ambient temperature. The average thickness of the as-grown Fe films was 200 nm. Sulfurization of such films has been done in the past in sealed quartz ampoules.^{13,14} The process reported there required vacuum evacuation of the ampoule “at least five times before sealing.”¹³ The films were then sulfurized for 20 h. The process used in our study was much simpler, taking much less time and incurring much less expense in a photovoltaic fabrication process.

In order to form pyrite, the Fe films were sulfurized in an open tube furnace at different temperatures and time durations in a sulfur and nitrogen atmosphere. The Fe on glass film along with elemental sulfur was placed in a graphite boat, similar to that discussed in a previous article on the selenization of Cu–In–B thin films.¹⁵ The graphite boat was placed in a quartz tube in a furnace. One end of the tube was vented to the atmosphere and, in order to prevent oxidation, a slow rate, 2.36 l/min, of N₂ gas was flowed over the structure. The furnace temperature was rapidly raised at a rate of 60 K/min to attain the annealing/sulfurization temperature and was typically kept there for 1 h; exceptions to this time are described in the text. The furnace heater was turned off and the temperature was allowed to attain room temperature before the sample was removed from the furnace.

After sulfurization, the thickness of the films increased to an average of 300 nm. X-ray diffraction (XRD) was the technique most relied on to determine the quality of the FeS₂ thin films. Only those films that had diffraction peaks that directly matched the powder diffraction standards were considered to be of the quality desired. Optical absorption of these films was then further studied using a Perkin Elmer Lambda 9

^{a)}Electronic mail: rsoukup@unl.edu

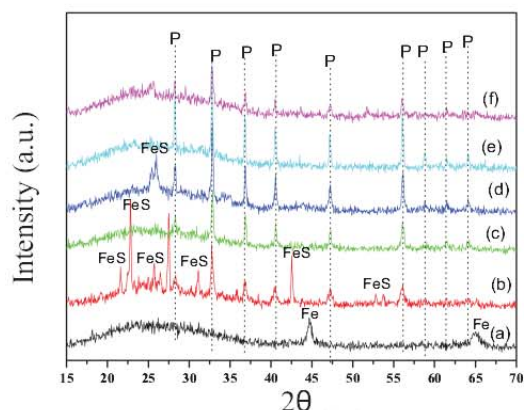


FIG. 1. (Color online) XRD patterns of the Fe films samples after sulfurizing and annealing for 1 h each: (a) Fe film, (b) 300 °C, (c) 350 °C, (d) 400 °C, (e) 450 °C, and (f) 500 °C. The peaks labeled P are for pyrite, FeS peaks are labeled as such, and the iron peaks for the unsulfurized material are labeled Fe.

UV/vis near infrared spectrometer. From these data, Tauc plots were made to determine the band gap. The scanning electron microscopy (SEM) was used to determine surface morphology and semiquantitative composition was obtained using Auger electron spectroscopy (AES). The resistivity and measure of Ohmic contact quality were the electronic measurements performed on these films.

III. RESULTS AND DISCUSSION

Figure 1 shows XRD patterns of the Fe film after sulfurization at different temperatures; all sulfurization times were 1 h long. For the as-deposited iron film grown at ambient temperature, two clear diffraction peaks were observed, indicating that the iron films grew with some order. A well defined (100) peak and weaker peak corresponding to the (200) planes were observed. Films sulfurized at the low end of the temperature range, 300 °C, show an x-ray diffraction peak corresponding to both FeS and FeS₂ (cubic phase) and possibly some other peaks. These results were as expected since the original Fe films had reasonable crystalline order. The dotted lines are FeS₂ (the ASTM card is 42-1340) and the locations of FeS peaks (the ASTM card is 02-1241) for the XRD patterns are listed. These powder diffraction results are shown for comparison of annealing/sulfurization process at different temperatures and different time intervals.

As can be seen, the sulfurizing temperatures of 350 °C and 450 °C yielded films with just cubic FeS₂. Interestingly enough, the intermediate temperature of 400 °C yielded a peak that can be attributed to FeS. This experiment was repeated with the same results. No explanation for this is known at this time. For the two temperatures of 350 °C and 450 °C, the XRD patterns gave no hints of other phases such as pyrrhotite, FeS, sulfur, or iron. In the case of sulfurization at 450 °C, the XRD peaks were very strong, narrow, and with high intensity. The XRD peaks can be indexed to sev-

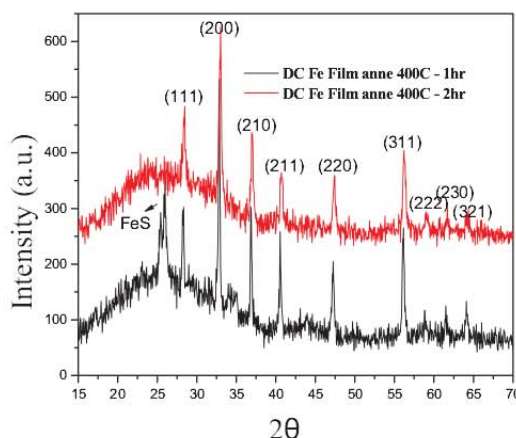


FIG. 2. (Color online) XRD patterns of the film samples processed at 400 °C after sulfurizing at constant temperature with different time durations illustrating that 2 h appears to be better for this temperature. The upper curve is from the sample grown for 2 h.

eral planes of the cubic phase of FeS₂ (see Fig. 2 for identification of these planes). Sulfurizing at $T=500$ °C results in additional phases reappearing and along with weaker pyrite reflections. The peaks at $2\theta=43^\circ$ and 52° are attributed to Troilite, another form of FeS.

With the exception of the film sulfurized at 350 °C, the trend is to obtain purer pyrite films at higher temperatures until 450 °C. Above this temperature, at least in steps of 50 °C, the films show additional FeS phases. The most likely cause for this is the high temperature decomposition of the pyrite.

Figure 2 shows XRD patterns of the dc Fe film sulfurized at 400 °C for 1 and 2 h durations. When sulfurizing at 400 °C for 2 h, the relatively broad peak at $2\theta=26.03^\circ$ has disappeared. Thus, it can be stated that this longer time duration at $T=400$ °C is sufficient to lead to the formation of the pyrite cubic phase and all the diffraction peaks match the cubic phase of FeS₂. The sulfurizing time dependence was examined for the film that yielded the best results for 1 h, $T=450$ °C. Figure 3 shows XRD profiles of the Fe film sulfurized at 450 °C for different time durations. Increasing the sulfurizing time for this temperature decreases the film quality as noted by the spreading and lowering magnitude of the peaks. This spreading and lowering indicates a smaller crystallite size that leads to more grain boundary recombination and lower current flow for photovoltaic applications. The ratios of peak intensities shown in Fig. 2 were measured where the most intense peak, which is the one from the (200) plane, is selected as the reference peak that was compared with the (210) and (311) peaks. The intensity ratio of (210) and (311) diffraction peaks to the (200) peak are almost same for the pyrite films sulfurized for time durations of 2 and 3 h. However, the peaks representing the (210) and (311) planes were broader at these longer sulfurization times than those with a 1 h processing time. The full width at half maximum

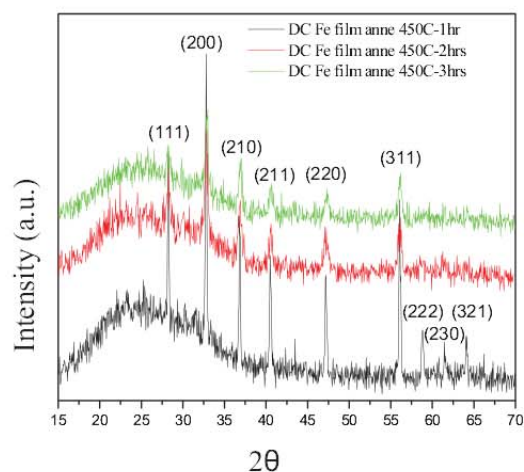


FIG. 3. (Color online) XRD patterns of the film samples processed at 450 °C after sulfurizing at constant temperature with different time durations illustrating that 1 h appears to be the best for this temperature. From bottom to top curves, the time durations are monotonically increasing in 1 h increments.

of the XRD peaks for the sulfurized Fe films increased with time duration. Other peaks, such as cubic pyrite phase diffraction peaks (222), (230), and (321), gradually disappear with increasing time duration.

Apparently, the additional time of sulfurization is needed at lower temperatures, but it is undesired at higher temperatures. The full width at half maximum of the diffraction peaks is an indicator of the film quality such that it is believed that the peak broadening is a consequence of smaller crystallite size. As stated above, for photovoltaic applications, the greater the crystallite size, the lower the grain boundary recombination and the higher the current output.

The morphologies of the pyrite thin films were studied in a field emission electron microscope. The films that exhibited the best XRD results were formed of small crystallites. Figure 4(a) is an example of the surface of a film, which was sulfurized at 450 °C for 1 h, and it appears to consist of small, nearly spherical crystallites. The surface shown in Fig. 4(b) is of another film sulfurized at 400 °C for 2 h. Although

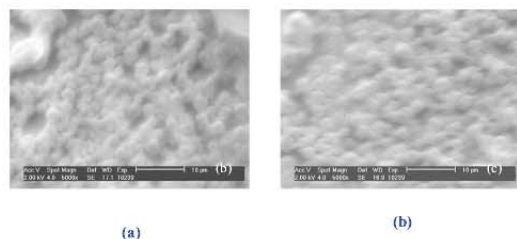


FIG. 4. (Color online) SEM morphologies showing nearly spherical surface crystals for the test films sulfurized from Fe layers at (a) 450 °C (1 h) and (b) 400 °C (2 h).

JVST A - Vacuum, Surfaces, and Films

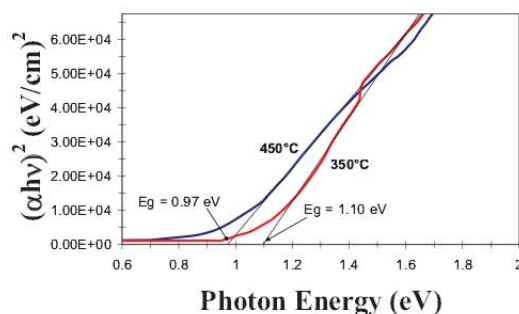


FIG. 5. (Color online) Tauc plots for the samples processed at 350 and 450 °C illustrating the optical gap is nearest the accepted value of 0.95 eV for the film processed at 450 °C.

the properties of the films are quite different, the surfaces are very similar. Figure 5 shows Tauc plots for the Fe films sulfurized at 350 and 450 °C, the two samples that exhibited only cubic FeS₂ peaks in the XRD measurements. The trend line for the linear portion of the curves for both films is also shown in Fig. 5. It can be seen that the Tauc band gap is as expected at 0.97 eV for the film sulfurized at 450 °C, but it is higher at 1.10 eV for the film processed at 350 °C. These results are just the opposite as that seen in sulfurized flash evaporated iron, where the apparent band gap decreases for lower processing temperatures.¹⁰ The transmission, T , and reflectance, R , of the photons at varying wavelengths were measured, and the absorption coefficients, α , of these films were determined in the spectral region of fundamental absorption by the following relationship:

$$\alpha = \frac{1}{d} \ln \left[\frac{1-R}{T} \right], \quad (1)$$

where d is the film thickness. The plot in Fig. 5 of $(\alpha h\nu)^2$ vs $h\nu$ for a direct band gap was used.⁷

The spectra for the various films showed clear absorption edges. This indicates that the films have a crystalline nature possibly with uniformity in optical properties. The band gap in sulfurized Fe thin films are somewhat higher than the values found in the literature,¹⁶ 1.13 eV (300 °C), 1.10 eV (350 °C), 1.18 eV (400 °C), 0.97 eV (450 °C), and 1.13 eV (500 °C), although the films processed at 450 °C all had band gaps very close to the accepted value of 0.95 eV. Again, the films processed at 450 °C appear to be superior to those processed at other temperatures such that the band gap more nearly matches that of pure pyrite. The experiments were repeatedly run with the same results, within a margin of error.

The chemical analysis of the films was carried out using AES. Of importance here is that the sulfurized Fe thin films exhibited AES depth profiling results where the signals were relatively constant throughout the entire film. Figure 6 is a depth plot of the Auger spectrum. The Fe:S ratio obtained from the spectrum when initially performed was not what was expected, i.e., 1:2, but this was an uncalibrated value. In

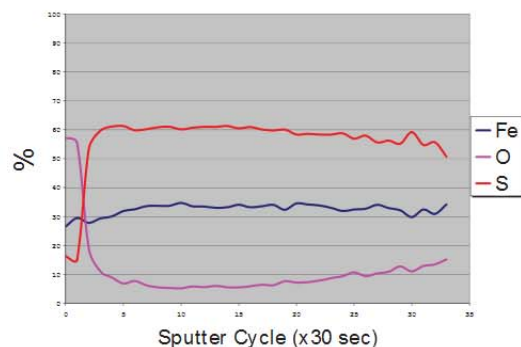


FIG. 6. (Color online) Depth profile AES spectrum of pyrite thin film grown at 450°C illustrating the uniformity of the composition and the possible presence of oxygen.

order to be assured that the samples were actually FeS_2 , a standard pyrite crystal of 99.9+ % pure FeS_2 was purchased. Knowing the content of the sample inserted into the Auger system allowed the sensitivity factors for Fe and S to be adjusted, so that the depth profile indicated that the pure pyrite sample was FeS_2 . It can be seen in Fig. 6 that the ratio of S to Fe in the film is 2:1 within experimental error, as expected. The film appears to contain a small amount of oxygen, but the amount is not known exactly. The oxygen level seen in Fig. 6 may just be actually lower, which appears as a consequence of the fact that in depth profiling in AES, oxygen can collect on the surface between sputtering runs. Oxygen also appeared, to a small degree, in the pure FeS_2 sample.

However, it is believed that oxygen is actually present in the films to some degree, but the actual level is unknown. In pyrite films created by nonvacuum processes in this laboratory,¹⁷ the films were *n*-type, which was attributed to possible oxygen content. In any case, the depth profile of the AES spectra shows that the as-deposited and pyrite thin films are quite uniform throughout the film and appear to have a S to Fe ratio of 2:1.

The Fe films that were sulfurized at 450°C (time duration of 1 h) and 400°C (time duration of 2 h) were all *p*-type semiconductors, as determined by the hot point probe technique. The *p*-type conductivity could be produced by an excess of Fe vacancies, which behave as acceptor states with energy levels near the valence band, although other possibilities cannot be disregarded. Electrical resistivity measurements have been made by applying the van der Pauw method. The room temperature resistivity of *p*-type pyrite thin films prepared at 450°C (1 h) was $0.50\ \Omega\text{ cm}$, and that at 400°C (2 h) was $0.58\ \Omega\text{ cm}$.

IV. OHMIC CONTACTS

It was shown by Schieck *et al.*¹⁸ that platinum makes a very good Ohmic contact to *p*-type iron pyrite, where Cu and Au both exhibited nonlinear current-voltage characteristics and Al and Pt were linear at currents in the microampere

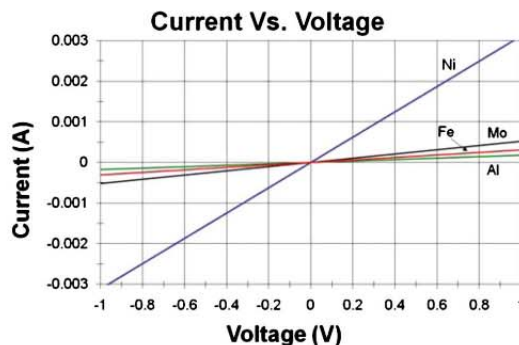


FIG. 7. (Color online) Linear *I-V* characteristics of the FeS_2 -metal contacts, Al, Mo, Fe, and Ni, illustrating that Ni yields the lowest resistance Ohmic contact.

range. However, the resistance of Pt was considerably lower than that of Al, $75\ \Omega$ for Pt as opposed to $667\ \Omega$ for Al. In order to find a good Ohmic contact for our films, which would be much less expensive than Pt, the following were chosen for study: Al, Mo, Fe, and Ni. The results of the current-voltage characteristics made using these metals on these films are shown in Fig. 7. Although each metal produced a linear current-voltage characteristic, Ni is seen to be the best with a resistance of $333\ \Omega$. This is not as good as Pt but is the best of this group, which is not surprising since the two metals are in the same column of the periodic table.

V. CONCLUSIONS

Pyrite (FeS_2) films have been prepared by thermal sulfurization of previously sputtered Fe thin films. Temperature (300 – 500°C) and sulfurization time have been the main variables utilized in this work. Formation of pyrite starts at 300°C with good crystallinity, but with additional phases present as seen using XRD. The XRD patterns show that sulfurization at 350 and 450°C yielded pure cubic phase pyrite films. The films produced at a sulfurization temperature of 350°C had XRD peaks that were somewhat less intense than those produced at 450°C . These two sulfurization temperatures yielded films with a better crystal structure, with only the pyrite form appearing in the XRD patterns. Pyrite films have very steep absorption coefficients versus $h\nu$ for photon energies just exceeding the band gap energy and their absorption edge (band gap) is 0.97 eV for sulfurization temperature of 450°C . This and an inexpensive Ohmic contact make these pyrite films a promising material for photovoltaic applications.

ACKNOWLEDGMENTS

This work is supported in part by the U.S. Department of Energy, Grant No. DE-FG36-08GO88007, the Nebraska Research Initiative, and the Department of Electrical Engineering at the University of Nebraska-Lincoln.

- ¹A. Ennaoui, S. Fiechter, Ch. Pettenkofer, N. Alonso-Vante, K. B. Ker, M. Bronold, Ch. Hopfner, and H. Tributsch, *Sol. Energy Mater. Sol. Cells* **29**, 289 (1993).
- ²A. Ennaoui, S. Fiechter, W. Jaegermann, and H. Tributsch, *J. Electrochem. Soc.* **133**, 97 (1986).
- ³Cyrus Wadia, A. Paulalivisatos, and Daniel M. Kammen, *Environ. Sci. Technol.* **43**, 2072 (2009).
- ⁴A. Yamamoto, M. Nakamura, A. Seki, E. L. Li, A. Hashimoto, and S. Nakamura, *Sol. Energy Mater. Sol. Cells* **75**, 451 (2003).
- ⁵D. M. Schleich and H. S. W. Chang, *J. Cryst. Growth* **112**, 737 (1991).
- ⁶B. Rezig, H. Dahman, and M. Kenzar, *Renewable Energy* **2**, 125 (1992).
- ⁷Y. Z. Dong, Y. F. Zheng, H. Duan, Y. F. Sun, and Y. H. Chen, *Mater. Lett.* **59**, 2398 (2005).
- ⁸G. Chatzitheodorou, S. Fiechter, R. Konenkap, M. Kunst, W. Jaegermann, and H. Tributsch, *Mater. Res. Bull.* **21**, 1481 (1986).
- ⁹L. Meng, J. P. Tu, and M. S. Liu, *Mater. Lett.* **38**, 103 (1999).
- ¹⁰I. J. Ferrer and C. Sanchez, *J. Appl. Phys.* **70**, 2641 (1991).
- ¹¹S. Nakamura and A. Yamamoto, *Sol. Energy Mater. Sol. Cells* **65**, 79 (2001).
- ¹²A. Gomes, J. R. Ares, I. J. Ferrer, M. I. da Silva Pereira, and C. Sanchez, *Mater. Res. Bull.* **38**, 1123 (2003).
- ¹³Liuyi Huang, Yanhui Liu, and Liang Meng, *J. Mater. Sci. Technol.* **25**, 237 (2009).
- ¹⁴X. F. Li, Y. Wang, and L. Meng, *Mater. Res. Bull.* **44**, 462 (2009).
- ¹⁵J. Olejnik, S. A. Darveau, C. L. Exstrom, R. J. Soukup, N. J. Ianno, C. A. Kamler, and J. L. Huguenin-Love, *Mater. Sci. Forum* **609**, 33 (2009).
- ¹⁶S. Fiechter, M. Birkholz, A. Hartmann, P. Dulski, H. Tributsch, and R. J. D. Tikkey, *J. Mater. Res.* **7**, 1829 (1992).
- ¹⁷P. Prabukanthan *et al.*, Proceedings of the 35th PVSC, 2010 (unpublished).
- ¹⁸R. Schieck, A. Hartmann, S. Fiechter, R. Konenkamp, and H. Wetzel, *J. Mater. Res.* **5**, 1567 (1990).